Journal of Food Biosciences and Technology,
Islamic Azad University, Science and Research Branch, Vol. 13, No. 3, 63-76, 2023
DOI: 10.30495/jfbt.2023.69768.10299 https://dorl.net/dor/20.1001.1.22287086.2023.13.3.6.6

The Effect of Core@Shell Nanoparticle Concentration on the Barrier Properties of Carboxymethyl Cellulose-Based Films

S. Tavakolian [a], ***H. Ahari*** [b,*], ***M. H. Givianrad*** [c], ***H. Hosseini*** [d]

[a] PhD Student of the Department of Food Science and Technology, Science and Research Branch, Islamic Azad University, Tehran, Iran.
[b] Professor of the Department of Food Science and Technology, Science and Research Branch, Islamic Azad University, Tehran, Iran.
[c] Assistant Professor of the Department of Chemistry, Science and Research Branch, Islamic Azad University, Tehran, Iran.
[d] Professorof the Faculty of Nutrition and Food Technology, Shahid Beheshti University of Medical Sciences, Tehran, Iran.

Received: 3 October 2022 Accepted: 22 May 2023

ABSTRACT: Nanotechnology is one of the critical elements in adjusting barrier properties in food packaging systems. In this study, it was tried to assess the effect of core@shell NPs (allotropes of Al_2O_3"γ,η,α" as core, and TiO_2 and SiO_2 as shell) on the barrier properties of carboxymethyl cellulose-based film including water vapor permeability, moisture absorption, and gas transmissionrate. The films were fabricated with 1, 3, and 5 %w/vof nanoparticles. The nanoparticles were analyzed from the viewpoint of morphology, crystallinity, and chemical structures. Based on the results, nanoparticles with TiO_2 as shells showed more crystallinity.Increasing the concentration of nanoparticles improved the barrier properties. This improvement was more significant in films withAl_2O_3@TiO_2 nanoparticles(alpha: 6.5 to 2.9, etha: 6.2 to 5.5, gama: 6 to 3.4 g/m.s.Pa).Based on the GTR results, nanoparticles with higher crystallinity could significantly block the gaspathways (alpha: 0.08 to 0.02, etha: 0.09 to 0.04, gama: 0.03 to 0.01%) and moisture pathways (alpha: 2.5 to 2, etha: 3 to 1, gama: 2 to 1 cm^3/m^2.d.bar).In conclusion, the core@shell type nanoparticles can be a good nominee for food packaging purposes.

Keywords: Alumina, Barrier Properties, Core-Shell Nanoparticle, Food Packaging, Nanocomposite.

Introduction

New food packaging systems (FPSs) introduced an attractive approach to the development of nanomaterials. Nanotechnology plays a vital role in developing active and smart food packaging systems (Souza and Fernando, 2016). A wide range of nanoparticles (NPs) is embedded within the packaging matrix to cause one or more functionalities for packaging. Based on the previous studies, NPs (e.g., Ag, Cu, Zn) revealed their potential as antibacterial, antioxidant, scavenger, filler agents, and nanosensors in FPSs. NPs also depicted their potential in adjusting the mechanical, thermal, physical, and chemical properties of FPSs (Jafarzadeh and Jafari, 2020).

One of the most important features of FPSs is their permeability toward gases

* Corresponding Author: dr.h.ahari@gmail.com

and vapor molecules. The majority of FPSs are based on biomaterial (both synthetic and natural) that own distinct efficacy in water vapor permeability, oxygen penetration, gas diffusion, Crsytalinity, transparency, thermal and mechanical stability, morphology, biodegradability, and biocompatibility (Reshmy *et al*., 2021). The presence of NPs (those with antibacterial activity and barrier properties) as filler demonstrated notable improvement in the mentioned properties. This improvement can be modified by i) type of NPs(eg., metal NPs, polymeric NPs, metal oxide NPs, metal-organic-frameworks, nanoemulsions, Nanotubes, nanorods, nanofibrils, encapsulated NPs) (Hosseinzadeh *et al*., 2020),ii) concentration of NPs (Peidaei *et al*., 2021), iii) way of NP embedding within the packaging matrix (Priyadarshi and Negi, 2017), and iv) way of NP synthesis (Espitia *et al*., 2012).Many studies reported the positive impact of NPs (those with antibacterial activity, scavenging, mechanical properties, and barrier properties) in improving the food's shelf life. Core@shell NPs own a higher surface area, thereby can leave more impact (e.g., antibacterial and antioxidant activity) in FPSs. In our previous study, Al_2O_3@SiO_2& Al_2O_3@TiO_2 NPs were embedded in CMC-based films and finally resulted in promoting the physical properties of the final films (Tavakolian *et al*., 2021).

The performance of FPSs depends on the size of the NPs and their uniform distribution and dispersion in the matrix. In spite of the positive effects of NPs, one of the main concerns about NPs and FPSs is developing low-cost and environmentally friendly FPSs. Increasing the NP content in FPSs on one hand can improve the FPS quality, while on the other hand can hazard human life due to the migration phenomenon (Ahari and Lahijani, 2021). Thereby, it is mandatory to optimize the NPs concentration in developing new FPSs that may be different for each type of NPs. However, the optimized concentration can be even different for a kind of NPs because of several factors such as the film thickness, employed biomaterial, film-making technique, food type, and addition of other additives.

The barrier properties of FPSs are critical for food shelf life enhancement. The concentration of NPs showed that can improve the barrier properties as nanofiller by blocking or prolonging the microchannels that exist in the polymeric film (Moghimi *et al*., 2018). As such, perishable food is protected from oxygen and other gases. NPs also make changes in their interface with the polymer matrix that have a significant effect on the barrier properties. In this regard, the type of NPs plays a significant role in the modification of the interfacial regions in the polymer matrix that causes a high gas permeability. However, it was also reported that the presence of NPs increases the crystallinity which can significantly reduce the crossing rate.

Core@shell NPs as one of the candidates in developing new FPSs has attracted the attention of scientists. Al_2O_3@SiO_2& Al_2O_3@TiO_2 are two NPs that due to their solid core and porous shell own a high surface area (Tavakolian *et al*., 2021). SiO_2 and TiO_2 are two NPs that showed good efficacy in FPSs as antibacterial agents with a high impact on the mechanical and barrier properties (Al-Tayyar *et al*., 2020). Employing both of them as core in the form of core@shell NPs showed more efficacy.

Carboxymethyl cellulose (CMC) is used as a stabilizer, thickener, and binder in the food industry and has a very good

effect on film formation and three-dimensional network structure. Also, since it is hydrophilic in reaction with alumina nanocomposites, it shows more resistance to moisture in food packaging. Thereby, in this study, it was tried to use CMC as the main material to produce the film.

In this study, it was tried to use Al_2O_3 as the core and SiO_2 and TiO_2as the shell and as an innovation, try to evaluate their concentration effect on the barrier properties of CMC-based film for food packaging purposes. The main goal of this study was to increase the properties of nanoparticles using the core and shell approach and also to investigate the use of low concentrations to reduce the amount of these nanoparticles in packaging.

Materials and Methods

- ***Materials***

Carboxymethyl cellulose (CMC) (Merck) was provided by Teb-Shahr Co. (Tehran, Iran). TiO_2NPs (150-200 nm) and SiO_2NPs (150-200 nm) were purchased from Armina Co. (Tehran, Iran). Ethanol, glycerol, ammonia, Al $(NO_3)_3.6H_2O$ (99% w/w), were in analytical grade (Merck)and purchased from the local supplier. All the chemicals were used without any further purification.

- ***Synthesis of nanomaterials***
- ***Synthesis of Al_2O_3***

6.07 g of Al $(NO_3)_3.6H_2O$ was dissolved in a 24 mL water: ethanol solution (3:1). Next, 12.29 mL ammonia (15 M) was added dropwise. Appearing a cloudy color, indicated the aluminum hydroxide formation. The final solution was heated in an oil bath for 24 h at 85 °C. Next, the produced gel was purified using distilled water and centrifuge (10000 rpm: 15 min) to remove the residual $Al(NO_3)_3$. The gel was then rinsed with ethanol to remove the remained water. Finally, the resulting gel was dried in an oven at 100°C for 24 h.

- ***Synthesis of α, η, γ-Al_2O_3***

The obtained powder from the previous part was placed in a furnace heated up to 1200, 750, and 500°C to synthesize α-Al_2O3, η-Al_2O_3, and γ-Al_2O_3 respectively. The heating rate was 2°C/min for 4 h. A high heating rate causes a rapid solvent removal that destroys cavities.

- ***Synthesis of α,γ,η-Al_2O_3@SiO_2 and α,γ,η-Al_2O_3@TiO_2***

First, Al_2O_3@TiO_2 and Al_2O_3@SiO_2 were synthesized according to section 2.2.1 under a little modification. To aim this, 6.07 g of Al $(NO_3)_3.6H_2O$ was dissolved in 24 mL of Water/Ethanol solution. Next, 0.25 g of TiO_2 NPs were dispersed under vigorous agitation at room temperature for 30 min, and then, the ammonia solution (15 M, 12.29 mL) was added dropwise. Then, the obtained mixture was heated in an oil bath at 85°C for 24 h. The resulting gel was dried at 100°C. The same procedure was repeated to synthesize Al_2O_3@SiO_2. Finally, γ-Al_2O_3@TiO_2,η-Al_2O_3@TiO_2, α-Al_2O_3@TiO_2 were synthesized by calcination of a desired amount of Al_2O_3@TiO_2 at 500, 750, and 1200°C for 4 h respectively. The same procedure was repeated to synthesize α,γ,η-Al_2O_3@SiO_2. The size of α,γ,η-Al_2O_3@SiO_2 NPs was in the range of 14-25 nm, and the size of α,γ,η-Al_2O_3@TiO_2 NPs was in the range of 25-50 nm.

- ***Preparation of films containing NPs***

1 g of CMC powder was dissolved in 100 mL distilled water at 80°C using a magnetic stirrer. Then, an appropriate amount of the synthesized NPs was added and dispersed under ultrasonication (100 W, 10 min) to finally reach solutions with

concentrations of 1, 3, and 5 %. Next, 0.5 g of glycerol (as a surfactant) was added dropwise to the solution and stirred for 30 minutes. The solution was degassed usingan ultrasonic bath for 5 min and then left at room temperature. Then, the solution was poured into a petri dish (d: 15 cm). The petri dish was placed in an oven at 40°C to remove the water content. After 24 h, the films were separated and stored in the refrigerator. The film's thickness was around 500 µ musing a micrometer.

- ***Field Emission Scanning Electron Microscopy analysis***

First, the synthesized NPs were coated using gold powder. Field Emission Scanning Electron Microscopy (FE-SEM, MIRA III, TESCAN Co.) was then employed to analyze the size and morphology of synthesized NPs (α,γ,η-Al_2O_3@SiO_2 NPs and α,γ,η-Al_2O_3@TiO_2 NPs).

- ***Fourier-transform infrared spectroscopy analysis***

Fourier transform infrared spectroscopy (FTIR, BRUKER TENSOR Ⅱ, Germany) was employed to analyze the chemical bonds of the synthesized NPs.

- ***X-ray Diffraction analysis***

X-ray diffraction (XRD) analysis was employed using Bruker D8 Advance X-ray diffractometer equipped with LYNXEYEXE-T detector. The diffractograms were collected in the 2θ range from 10 to 80° with a scanning rate of 2 °/min.The information about nanoparticles was compared with the standard data in the ICCD-PDF2 / PDF4 software library (created in 2004).

- ***Moisture absorption (MA)***

The prepared CMC-based films were completely dried at 40°Cand then cooled down in a desiccator before usage and then weighed (W1). Then, the films were immersed in water for 24 h at room temperature. Finally, films were pulled out from the water, the residual water was removed, and weighed (W2) (Shen and springer, 1976).

- ***Water Vapor Permeability (WVP)***

Gravimetric techniques were employed to measure WVP according to standard No. ASTM E96-95. 10 mL of distilled water was poured into a glass vial (with a specific diameter) to create 100% humidity and then a piece of film with the area of "A"hascovered the lid of the vial and sealed with plastic washers and glue and the vial was weighed (W1). It was then placed in a desiccator and changes in their weight were recorded by weighing them (W2) after a specific period Δt.

The WVP was calculated by the following equations (1) and (2):

$$WVPR = \frac{\frac{\Delta m}{\Delta t}}{A} \quad (1)$$

In which,
WVPR: WVP rate (g/s.m^2)
Δm: gram
Δt: time (s)
A: area (m^2)

$$WVP = \frac{WVPR}{P} \times X \quad (2)$$

In which, WVP is reported by (g/s.m·Pa), P: Pure water vapor pressure at 25 °C (Pa), X: the film thickness (m)

- ***Gas transmission rate (GTR)***

GTR was determined by measuring the volume of gas diffused through the film according to ASTM D1434 standard, by employing GDP-C gas permeability tester (Coesfeld Meteriatest, Germany) (Mrkic *et al*. 2006).

- ***Statistical analysis***

GraphPad Prism 9and analysis of variance (ANOVA) were employed to analyze the results statistically. The results were reported as mean ± standard deviation. and P <0.05 was considered a significant difference.

Results and Discussion

In this study, both TiO_2 and SiO_2 NPs (as a shell) were coated on three allotropes of Al2O3 (as core) to synthesize distinct core@shell NPs including α-Al_2O_3, α-Al_2O_3@SiO_2, α-Al_2O_3@TiO_2,η-Al_2O_3, η-Al_2O_3@SiO_2, η-Al_2O_3@TiO_2,γ-Al_2O_3, γ-Al_2O_3@SiO_2, γ-Al_2O_3@TiO_2. The microscopic images of calcinated alumina were presented in Figure.1 too. Figure. 1 also shows the microscopic images of the synthesized NPs. As can be seen in Figure. 1 (a type) the allotropes of alumina werein the form of plates and microparticlesthat seem to be brittle. However, these particles were dispersed in water easily. Figure. 1 (b type) depicts the core@SiO_2 NPs. As it can be seen, about all allotropes NPs seem to be created but aggregated the reason turns back to the calcination process. The same approach is interpreted for core@TiO_2 NPs. Based on the SEM images, it can be concluded that a significant difference is detectable by comparing alumina appearance before and after NP synthesis.

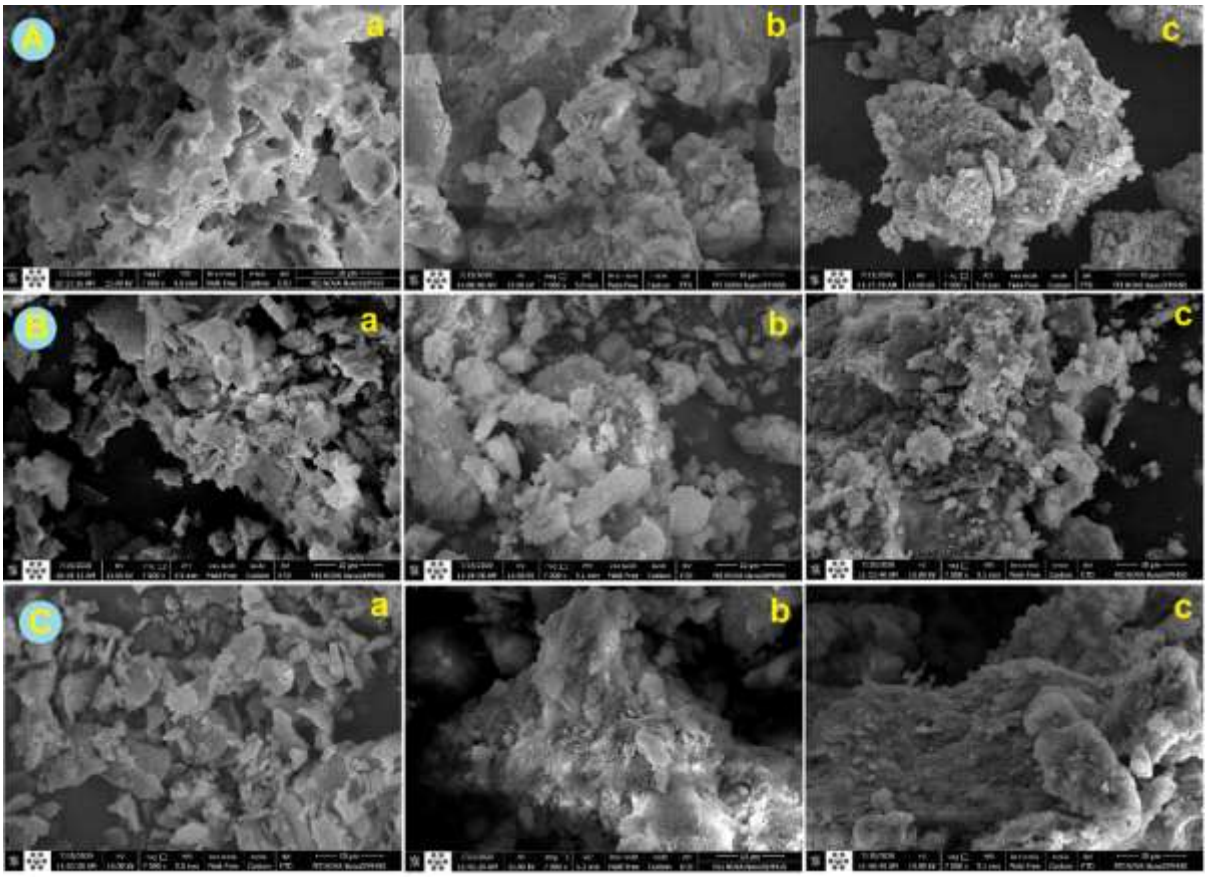

Fig. 1. FE-SEM images for **A)** a: α-Al_2O_3; b: α -Al_2O_3@SiO_2; c: α -Al_2O_3@TiO2, **B)** a: η-Al_2O_3; b: η -Al_2O_3@SiO_2; c: η -Al_2O_3@TiO_2, **C)** a: γ-Al_2O_3; b: γ-Al_2O_3@SiO_2; c: γ-Al_2O_3@TiO_2.

FTIR analysis gives critical information about the chemical bands by which the materials and synthesis of new products are detectable.

Figure. 2–Billustrates the FTIR spectra for all alumina allotropes(400–4000 cm^{-1}) that all Followed the same trend with similar peaks at 450 cm^{-1}, 592 cm^{-1}, 650 cm^{-1}, 700 cm^{-1}, 900 cm^{-1}, 1380 cm^{-1}, 1641 cm^{-1}, and 3450 cm^{-1}. The peaks that appeared at 650-450 $cm^{-1}$are attributed to the strength vibrations of the octahedral AIO6 group (Prashanth, Raveendra *et al*. 2015). The peaks at 700 cm^{-1} and 900 cm^{-1} belong to the strength vibrations of tetrahedral AIO4 species. The peak at 1380 cm^{-1}belongs to the OH group (Farahmandjou and Golabiyan, 2015).

Figure. 3 shows the FTIR spectra for core@SiO_2 and core@TiO_2NPs respectively in the range of 400–4000 cm^{-1}. As can be seen in Figure. 3-A, a similar trend was reported for all of the core@SiO_2 NPs. The small band that appeared at 459 cm^{-1} is attributed to the Si-O-Si bond that confirms the presence of SiO_2. By comparing this peak in Figure. 3-A with that of SiO_2 in Figure. 2-A, it is clear that the peak shifted to 466 cm^{-1} after core@SiO_2 production. The appearing spectra of SiO_2 in 1220–950 cm^{-1}confirm the formation of the core@SiO_2 NPs(Ding *et al*., 2012).

Regarding the core@TiO_2 (Figure. 3-B), Comparing Figure. 2-B and Figure.3-B (TiO_2 spectrum), the appropriate transmittance of the peak at 483 cm^{-1}decreased, and a wide band at 1200 cm^{-1}appeared that approves the interaction between alumina and shell (TiO_2). This interaction happened extensively about η-Al_2O_3@TiO_2 compared to.α-Al_2O_3@TiO_2 and γ-Al_2O_3@TiO_2.

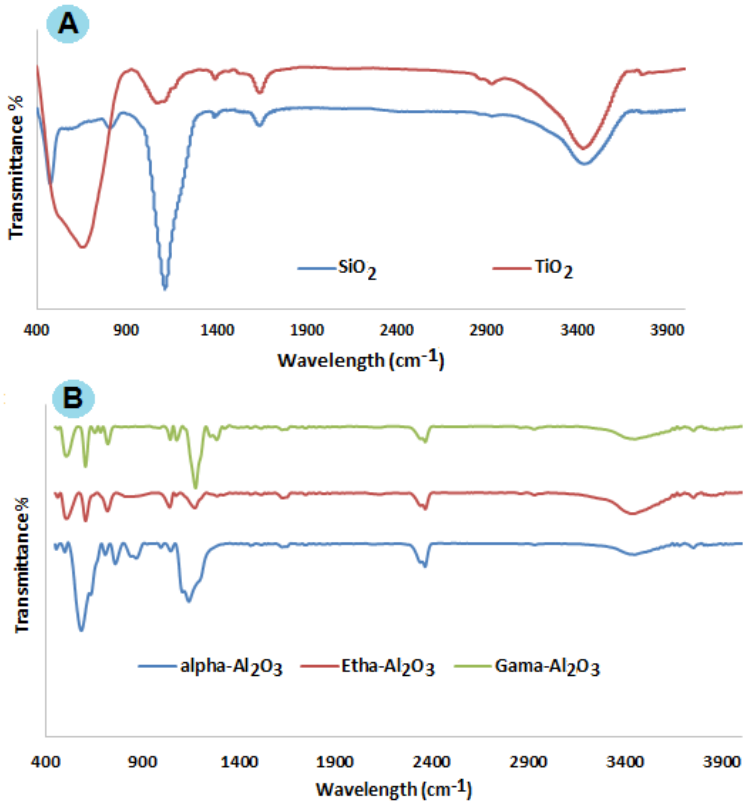

Fig. 2. FTIR spectrum for A) SiO_2 and TiO_2 NPs, B) different allotropes of alumina.

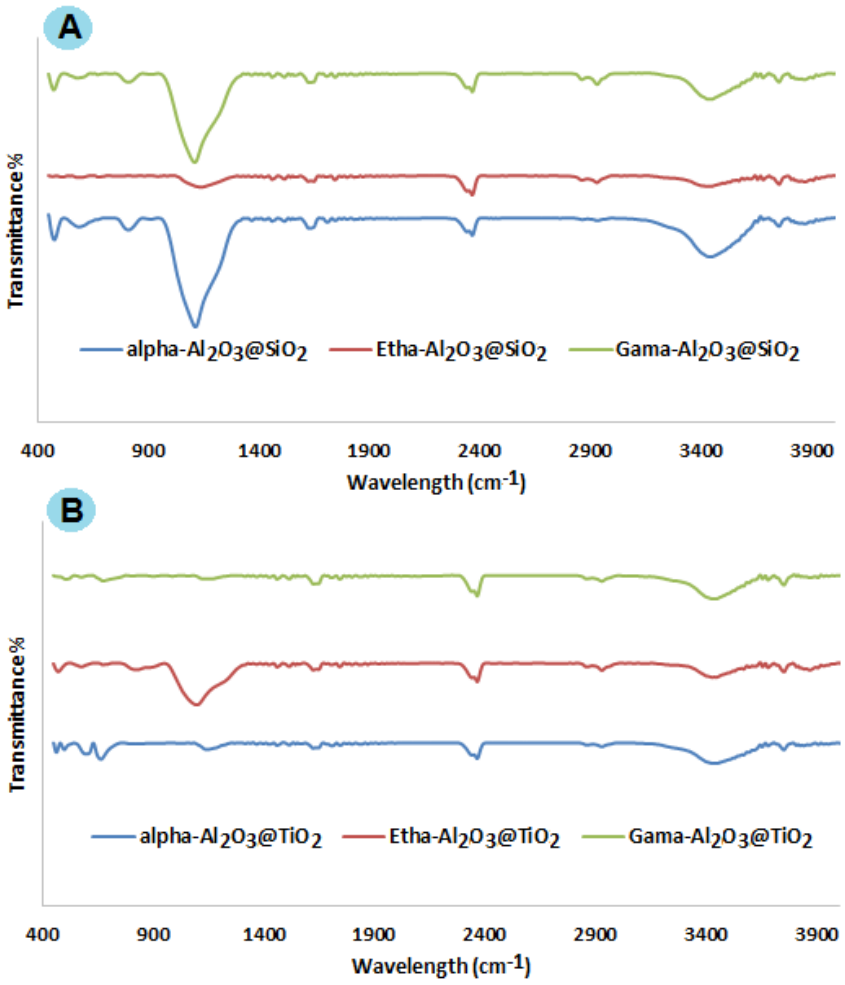

Fig. 3. FTIR spectrum for A) NPs with SiO_2, B) Nps with TiO2, as the shell.

The crystal structure of a material is deeply related to its atoms and their arrangement in its structure, which XRD pattern is a good technique for structural analysis. In general, two distinct types of materials exist: i) Amorphous Materials: Those materials like liquids in which the atoms are randomly arranged without any ordered network, ii)Crystalline Materials: the materials with atoms in an ordered arrangement with a spatially repeated pattern in three directions. SiO_2 and TiO_2 have a morph structures. Notably, when they are coated on the surface of other NPs, they alter the XRD pattern and decrease the intensity of the relevant peaks. This phenomenon is known as a sign of a successful coating. Nevertheless, both SiO_2 and TiO_2 can obtain crystalline structure by thermal annealing above 350 ˚C that means can show a crystalline pattern. When the materials are heated up to high degrees, the reconstruction of atoms and phase changes occur.

Figure. 4-A shows the IR spectra of TiO_2 and SiO_2. Considering SiO_2, two bands at 800 and 1097 cm^{-1} are attributed to the Si–O–Si bending vibrations and asymmetric stretching, respectively (Mohammadi et al., 2019).The spectra related to the 1074 and 1220 cm^{-1} are related to the asymmetric stretching modes of Si-O-Si (Ewing *et al.*, 2014). Considering TiO_2 NPs, the peak that

appeared in the range of 1000-400 $cm^{-1}$is attributed to the bending vibration of Ti–O and O–Ti–O bonds (Catauro *et al.*, 2018).For instance, the peak at 483 cm^{-1} is known for the Ti-O vibrations, and Ti-O flexural vibrations appeared at 1630 cm^{-1} (Choudhury and Choudhury 2012). When the materials are heated up to high degrees, the reconstruction of atoms and phase changes occur.

As can be seen in Figure. 4-A, two phases of Al_2O_3at 2Θ equal 67˚, 45˚,38˚, and SiO_2at 2Θ equal 22˚appeared (Okuno, Zotov *et al.* 2005). Considering all allotropes, wide peaks appeared corresponding which depicts the amorphous structure of core@SiO_2 NPs (Kusumawati *et al.*, 2018). The obtained results matched the standard SiO_2 card pattern from the software library (No. PDF 01-086-1628) (Nallathambi *et al.*, 2011). α-Al_2O_3@SiO_2 NPs depicted a sharp peak at 2Θ equal to 67˚ which in comparison to the other allotropes it can be inferred that no SiO_2coating happened to some Al_2O_3 and that is why this peak is sharp while for other allotropes it is wide. Considering Figure. 4-B, Al_2O_3 and TiO_2 phases appeared at the angels of 26˚, 36 ˚, 57 ˚, 68 ˚and 28˚, 38˚, 48˚, 54.2˚, 55.3, 63.8˚ respectively (Ali *et al.*, 2018). By comparing the spectrum of all allotropes it can be seen that all of them gave similar patterns but different in some angles. The amorphous structure of TiO2 turns to crystalline type at high temperatures (Lin *et al.*, 2019). Thereby, the presence of sharp peaks can confirm the coating process. By the way in general, core@TiO_2 NPs showed more crystalline structure than core@SiO_2 NPs. The results matched the standard TiO_2 card pattern from the software library (No. PDF 04-006-9240).

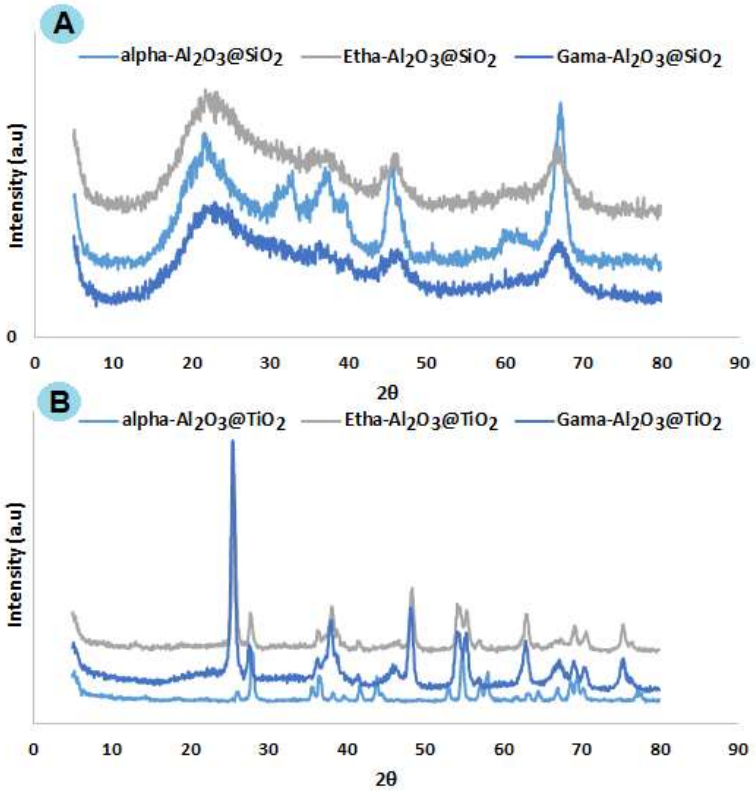

Fig. 4. XRD patterns for A) NPs with SiO_2, B) Nps with TiO2, as the shell.

The concentration of NPs plays a distinguished role in adjusting the mechanical behavior, thermal resistance, physicochemical properties, and barrier properties of FPSs(Shankar *et al*., 2019). Figure.5 provides information about the effect of core@shell NPs concentration on the barrier properties (WVP, MA, and GTR) of the CMC-based films. Considering the WVP parameter (Figure. 5-A), as it can be seen, WVP decreased by increasing the concentration of NPs from 1% to 5% in all groups. Considering film with 1 and 3% of NPs, γ-Al_2O_3@TiO_2 showed more reduction in WVP in comparison with all NPs ($P < 0.05$). The rational reason can be attributed to the more crystalline phase of γ-Al_2O_3@TiO_2 (based on the XRD results). No significant difference was observed between η-Al_2O_3@SiO_2 and η-Al_2O_3@TiO_2 ($P>0.05$). In this regard, it can be predicted that they might have similar nanometric features. Comparing all groups, the most WVP reduction belonged to α-Al_2O_3@SiO_2 (5%) which made a significant difference compared to other NPs ($P<0.01$). It seems that a higher concentration of this NP is needed. Surprisingly, α-Al_2O_3@SiO_2 demonstrated a better impact on WVP in comparison with α-Al_2O_3@TiO_2 ($P < 0.05$). In contrast with γ-Al_2O_3@SiO_2, γ-Al_2O_3@TiO_2 showed more reduction in WVP for 1% and 3% ($P < 0.05$), while no significant difference was observed in 5% ($P>0.05$). α-Al_2O_3@TiO_2 depicted less effect on WVP considering all concentrations.

Based on previous studies, increasing the concentration of NPs does not always decrease WVP. For instance, Shankar and her colleagues reported that the decrease in WVP of the gelatin-based film depends on the concentration of NPs, which decreases uniformly with the increasing concentration of NPs (Shankar *et al*., 2019). This is while others reported against it. For example, Voon *et al*. incorporated nanoclay and SiO_2 NPs in Gelatin films and reporteda significant reduction in WVP (Voon *et al*., 2012). Shankar and his colleagues reported WVP enhancement of FPSs by embedding metal NPs (Shankar *et al*., 2015). In another study, Yang and his colleagues used nanocrystalline cellulose in gelatin film and showed that WVP decreased by increasing the concentration of NPs (Yang *et al*., 2018). By comparing the previous studies, it is believed that NPs can decrease WVP by increasing the crystallinity of biopolymers or by reducing free hydrophilic groups such as OH and NH. It seems that core@shell NPs in this study could reduce WVP by increasing the crystallinity and creating bonds with hydrophilic groups of CMC (Trifol *et al*., 2020).

In the case of MA, as it can be seen in Figure 5-B, the most MA improvement belonged to the γ-Al_2O_3@SiO_2 (5%) ($P<0.01$), and the less MA improvement was attributed to the γ-Al_2O_3@TiO_2 (5%) ($P>0.05$). In general, among the films with 1% NPs, the most and the less MA reduction were attributed to γ-Al_2O_3@SiO_2 ($P<0.05$) and η-Al_2O_3@SiO_2 ($P<0.05$) respectively. Considering films with 3% NPs, α-Al_2O_3@SiO_2, and γ-Al_2O_3@SiO_2 showed the most reduction in MA ($P < 0.05$), while the lowest MA improvement belonged to η-Al_2O_3@SiO_2. Considering the films with 5% NPs, γ-Al_2O_3@TiO_2 showed the most MA adjustment ($P<0.01$), while γ-Al_2O_3@TiO_2 demonstrated the least MA reduction ($P>0.05$).The least MA belonged to the films incorporated withγ-Al_2O_3@shell NPs the rational justification behind this is the high temperature of calcination that resulted in more crystalline and small NPs. By comparing all groups, it can be

predicted that based on the employed NPs, increasing the concentration of NPs could reduce or increase the MA level. Similar to WVP, distinct factors can alter MA changes. It means that each of the NPs needs more study to find the optimized concentration.

Based on previous studies, biomaterials due to high water sorption have limitations in food packaging. The moisture content of the FPSs is influenced by relative humidity. The addition of NPs showed an improvement in MA. For instance, Othman *et al*. fabricated starch/chitosan NPs films for food packaging. They reported that the addition of chitosan NPs improved both water sorption and mechanical properties (Othman, Kechik *et al*. 2019). Similar reports were published regarding other types of NPs including metal NPs (Jayakumar *et al*., 2019). Considering core@shell NPs and based on the results, necessarily increasing the concentration of NPs does not guarantee the MA improvement and crystallinity and size of NPs can be effective. Similarly, Trifol and his colleagues demonstrated a slight improvement in water vapor sorption (Trifol *et al*., 2020).

Considering GTR, the most GTR reduction belonged to γ-Al_2O_3@SiO_2 andγ-Al_2O_3@TiO_2 NPs with no significant difference ($P > 0.05$). However, films with 3% and 5 % of γ-Al_2O_3@shell NPs showed the least but similar GTR levels ($P>0.05$). Considering the films with η -Al_2O_3@shell NPs, no significant difference was observed ($P > 0.05$), except for the concentration of 5%. Similarly, no significant difference was observed between α-Al_2O_3@SiO_2 and α-Al_2O_3@TiO_2 ($P>0.05$), except for the concentration of 1%. Thereby, it can be inferred that η -Al_2O_3@shell had a higher potential in preventing gas diffusion. However, the efficacy of γ-Al_2O_3@TiO_2 was slightly higher than γ-Al_2O_3@SiO_2.

In general, increasing the concentration of NPs improved GTR. Two important factors that determine the rate of transfer or permeability of oxygen through packaging materials are oxygen solubility and the rate of oxygen diffusion in the polymer matrix (Fasake, Shelake *et al*. 2021). The solubility of oxygen depends on the chemical relationship and the rate of diffusion is influenced by the microstructure of polymer and additives (Roda *et al*., 2019). By the way, the size of NPs and their surface area play a vital role in blocking the pathways, creating more zig-zag microchannels, or blocking the active sites. The issue of crystallinity can also be considered for the polymer matrix too. However, focusing on NPs, the addition of NPs increases the crystallinity degree of the polymer matrix and decreases gas permeability. Ramos and his colleagues reported the positive effect of NPS in different concentrations on reducing GTR (Ramos *et al*., 2014). In another study, the potential of NPs was approved by Li *et al*. (Li *et al*., 2018). In a similar study, PLA/TiO_2 (1, 3, and 5wt %) nanocomposite was fabricated by the casting technique, and it was reported that GTR had an inverse relationship with TiO_2 Concentration (Ali and Noori, 2014).

In general, increasing the concentration of NPs can not necessarily reduce or increase the barrier properties of the films, and the control of these properties can depend on factors such as the polymer material, film thickness, NPs type, and the interaction between the NPs and the film.

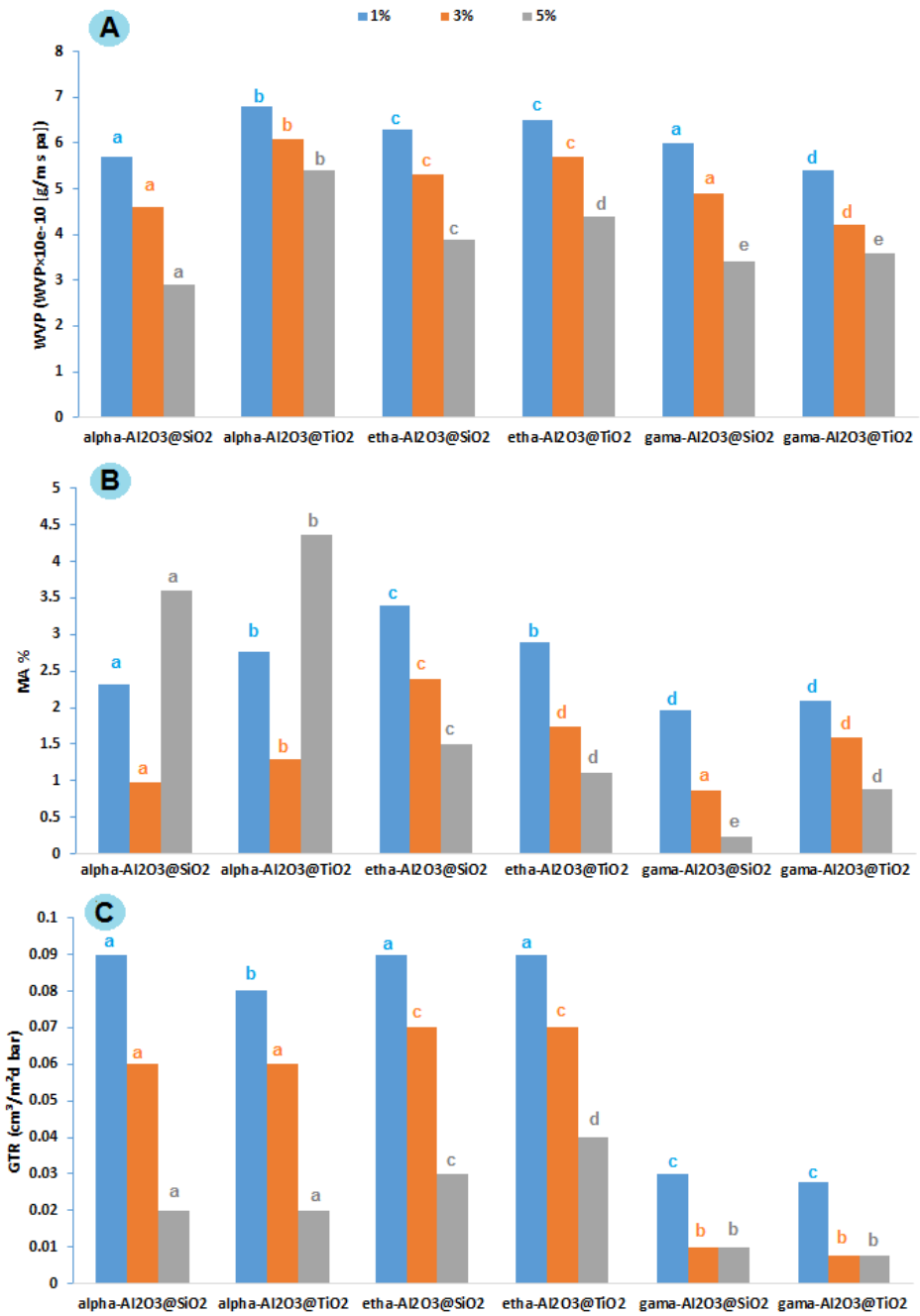

Fig. 5. The effect of the concentration (%) of core@shell NPs on A) water vapor permeability (g/m.s.Pa), B) moisture absorption (%), and C) gas transmission rate (cm^3/m^2.d.bar).

But, as the practical implication, in the case of barrier properties, the presence of NPs (any kind) showed that have barrier properties, and based on this research it was found that employing the core & shell approach can improve the barrier properties of NPs.

Conclusion

In this study, it was tried to study the effect of the concentration ofthree allotropes of Al_2O_3@TiO_2 and Al_2O_3@SiO_2 NPs on the barrier properties of the CMC-based films for food packaging purposes. In general, the addition of both NPs and increasing their

concentration improved the barrier properties. The results demonstrated that films containing NPs with more crystallinity showed better barrier properties. To sum up, using the core and shell approach can enhance the barrier potential of NPs compared to their simple form.

As are commendation, it is recommended to study these NPs in synthetic polymer-based films and natural polymer-based films. Their hybrid form is another idea that can be considered for more studies. core and shell NPs own a high surface area and they might be a good candidate to load antibacterial agents like herbal extracts. This recommendation may enhance their antibacterial activity.

References

Ahari, H. & Lahijani, L. K. (2021). Migration of Silver and Copper Nanoparticles from Food Coating. Coatings, 11(4), 380.

Al-Tayyar, N. A., Youssef, A. M. & Al-Hindi, R. R. (2020). Antimicrobial packaging efficiency of ZnO-SiO2 nanocomposites infused into PVA/CS film for enhancing the shelf life of food products. Food Packaging and Shelf Life, 25, 100523.

Ali, A. P. A. S., Mohammed, A. J. & Saud, H. R. (2018). Hydrothermal synthesis of TiO2/Al2O3 nanocomposite and its application as improved sonocatalyst. International Journal of Engineering & Technology, 7(4.37), 22–25.

Ali, N. A. & F. T. M. Noori (2014). Gas barrier properties of biodegradable polymer nanocomposites films. Chemistry and Materials Research, 6 (1).

Ding, H. L., Zhang, Y. X., Wang, S., Xu, J. M., Xu, S. C. & Li, G. H. (2012). Fe3O4@SiO2 core/shell nanoparticles: The silica coating regulations with a single core for different core sizes and shell thicknesses. Chemistry of Materials, 24(23), 4572–4580.

Espitia, P. J. P., Soares, N. d. F. F., dos Reis Coimbra, J. S., de Andrade, N. J., Cruz, R. S. & Medeiros, E. A. A. (2012). Zinc oxide nanoparticles: synthesis, antimicrobial activity and food packaging applications. Food and Bioprocess Technology 5(5), 1447-1464.

Farahmandjou, M. & Golabiyan, N. (2015). Solution combustion preparation of nano-Al2O3: Synthesis and characterization. Transp Phenom Nano Micro Scales, 3(2), 100–105.

Fasake, V., Shelake, P. S., Srivastava, A. & Dashora, K. (2021). Characteristics of Different Plastic Materials, Properties and their Role in Food Packaging. Current Nutrition & Food Science, 17(9), 944-954.

Hosseinzadeh, S., Partovi, R., Talebi, F. & Babaei, A. (2020). Chitosan/TiO2 nanoparticle/Cymbopogon citratus essential oil film as food packaging material: Physico-mechanical properties and its effects on microbial, chemical, and organoleptic quality of minced meat during refrigeration. Journal of Food Processing and Preservation, 44(7), e14536.

Jafarzadeh, S. & Jafari, S. M. (2020). Impact of metal nanoparticles on the mechanical, barrier, optical and thermal properties of biodegradable food packaging materials. Critical Reviews in Food Science and Nutrition, 1-19.

Jayakumar, A., Heera, K., Sumi, T., Joseph, M., Mathew, S., Praveen, G., Nair, I. C. & Radhakrishnan, E. (2019). Starch-PVA composite films with zinc-oxide nanoparticles and phytochemicals as intelligent pH sensing wraps for food packaging application. International Journal of Biological Macromolecules, 136, 395-403.

Kusumawati, D. H., Primary Putri, N., Hidayat, N., Taufiq, A. & Supardi, Z. A. I. (2018). Synthesis and characterization of γ-Al 2 O 3/SiO 2 composite materials. Journal of Pharmaceutical Health Care and Sciences, 1093(1), 012015.

Li, X., Bandyopadhyay, P., Nguyen, T. T., Park, O. K. & Lee, J. H. (2018). Fabrication of functionalized graphene oxide/maleic anhydride grafted polypropylene composite film with excellent gas barrier and anticorrosion properties. Journal of Membrane Science, 547, 80-92.

Lin, J., Ren, W., Li, A., Yao, C., Chen, T., Ma, X., Wang, X. & Wu, A. (2019). Crystal–amorphous core–shell structure synergistically enabling TiO2 nanoparticles' remarkable SERS sensitivity for cancer cell imaging. ACS Applied Materials & Interfaces, 12(4), 4204-4211.

Moghimi, N., Sagi, H. & Park, S. I. (2018). Leakage analysis of flexible packaging: Establishment of a correlation between mass extraction leakage test and microbial ingress. Food Packaging and Shelf Life, 16, 225-231.

Nallathambi, G., Ramachandran, T., Venkatachalam, R. & Palanivelu, R. (2011). Effect of silica nanoparticles and BTCA on physical properties of cotton fabrics. Materials Research, 14(4), 552–559.

Okuno, M., Zotov, N., Schmücker, M. & Schneider, H. (2005). Structure of SiO2–Al2O3 glasses: Combined X-ray diffraction, IR and Raman studies. Journal of Non-Crystalline Solids, 351(12), 1032–1038.

Othman, S. H., Kechik, N. R. A., Shapi'i, R. A., Talib, R. A. & Tawakkal, I. S. M. A. (2019). Water Sorption and Mechanical Properties of Starch/Chitosan Nanoparticle Films. Journal of Nanomaterials, 3843949.

Peidaei, F., Ahari, H., Anvar, S. A. A. & Ataee, M. (2021). Nanotechnology in Food Packaging and Storage: A Review. Iranian Journal of Veterinary Medicine, 15(2), 123-153.

Prashanth, P. A., Raveendra, R. S., Hari Krishna, R., Ananda, S., Bhagya, N. P., Nagabhushana, B. M., Lingaraju, K. & Raja Naika, H. (2015). Synthesis, characterizations, antibacterial and photoluminescence studies of solution combustion-derived α-Al2O3 nanoparticles. Journal of Asian Ceramic Societies, 3(3), 345–351.

Mrkić, S., Galić, K., Ivanković, M., Hamin, S. & Ciković, N. (2006). Gas transport and thermal characterization of mono-and di-polyethylene films used for food packaging. Journal of Applied Polymer Science, 99(4), 1590–1599.

Priyadarshi, R. & Negi, Y. S. (2017). Effect of varying filler concentration on zinc oxide nanoparticle embedded chitosan films as potential food packaging material. Journal of Polymers and the Environment, 25(4), 1087-1098.

Ramos, M., Jiménez, A., Peltzer, M. & Garrigós, M. C. (2014). Development of novel nano-biocomposite antioxidant films based on poly (lactic acid) and thymol for active packaging. Food Chemistry, 162, 149-155.

Reshmy, R., E. Philip, E., Madhavan, A., Sindhu, R., Pugazhendhi, A., Binod, P., Sirohi, R., Awasthi, M. K., Tarafdar, A. & Pandey, A. (2021). Advanced biomaterials for sustainable applications in the food industry: Updates and challenges. Environmental Pollution, 283, 117071.

Roda, A., Matias, A. A., Paiva, A. & Duarte, A. R. C. (2019). Polymer science and engineering using deep eutectic solvents. Polymers, 11(5), 912.

Shankar, S., Teng, X., Li, G. & Rhim, J. W. (2015). Preparation, characterization, and antimicrobial activity of gelatin/ZnO

nanocomposite films. Food Hydrocolloids, 45, 264-271.

Shankar, S., Wang, L. F. & Rhim, J. W. (2019). Effect of melanin nanoparticles on the mechanical, water vapor barrier, and antioxidant properties of gelatin-based films for food packaging application. Food Packaging and Shelf Life, (21), 100363.

Shen, C. H. & Springer, G. S. (1976). Moisture absorption and desorption of composite materials. Journal of Composite Materials, 10(1), 2–20.

Souza, V. G. L. & Fernando, A. L. (2016). Nanoparticles in food packaging: Biodegradability and potential migration to food—A review. Food Packaging and Shelf Life, 8, 63–70.

Tavakolian, S., Ahari, H., Givianrad, M. H. & Hosseini, H. (2021). Improving the Barrier Properties of Food Packaging by Al 2 O 3@ TiO 2 & Al 2 O 3@ SiO 2 Nanoparticles. Food and Bioprocess Technology, 1-14.

Trifol, J., Plackett, D., Szabo, P., Daugaard, A. E. & Giacinti Baschetti, M. (2020). Effect of Crystallinity on Water Vapor Sorption, Diffusion, and Permeation of PLA-Based Nanocomposites. ACS Omega, 5(25), 15362-15369.

Voon, H. C., Bhat, R., Easa, A. M., Liong, M. T. & Karim, A. A. (2012). Effect of Addition of Halloysite Nanoclay and SiO_2 Nanoparticles on Barrier and Mechanical Properties of Bovine Gelatin Films. Food and Bioprocess Technology, 5(5), 1766-1774.

Yang, S., Li, H. & Sun, H. (2018). Preparation of gelatin-based films modified with nanocrystalline cellulose. Iranian Polymer Journal, 27(9), 645-652.